

## SELECTIVE N<sub>2</sub>O GAS SENSING PERFORMANCE OF Y-MODIFIED B<sub>12</sub>N<sub>12</sub> NANOCAGE: A DFT APPROACH

## DESEMPENHO SELETIVO NA DETECÇÃO DO GÁS N<sub>2</sub>O POR NANOGAIOLA B<sub>12</sub>N<sub>12</sub> MODIFICADA COM Y: UMA ABORDAGEM DFT

**Wellington da Conceição Lobato do Nascimento**

PhD student in Chemistry – Federal University of Maranhão – UFMA, Brazil

Email: [wellington.conceicao@discente.ufma.br](mailto:wellington.conceicao@discente.ufma.br)

**Natanael de Sousa Sousa**

PhD in Chemistry – Federal University of Maranhão – UFMA, Brazil

Email: [83.natan@gmail.com](mailto:83.natan@gmail.com)

**Francivaldo Santos da Silva**

PhD student in Chemistry – Federal University of Maranhão – UFMA, Brazil

Email: [francivaldoss@gmail.com](mailto:francivaldoss@gmail.com)

**Felipe Anderson Silva de Aquino**

Master's degree in Materials Engineering - Federal Institute of Maranhão – IFMA, Brazil

Email: [aquinofelipe444@gmail.com](mailto:aquinofelipe444@gmail.com)

**Adeilton Pereira Maciel**

Department of Chemistry - Federal University of Rio Grande of Norte – UFRN, Brazil

Email: [adeilton.maciel@ufrn.br](mailto:adeilton.maciel@ufrn.br)

### Graphical Abstract



## Abstract

The emission of nitrous oxide ( $N_2O$ ) represents a serious environmental challenge due to its contribution to ozone layer depletion. In this work, density functional theory calculations with dispersion correction (DFT-D3), employing the B3LYP functional and the LanL2DZ basis set, were carried out to investigate the adsorption of  $N_2O$  on pristine and yttrium-modified  $B_{12}N_{12}$  nanocages. Geometric, electronic, and energetic parameters were analyzed, as well as the electronic sensitivity of the systems toward gas adsorption. The  $Y@b_{66}$  nanocage exhibited the largest variation in the energy gap ( $\Delta E_{gap} = 38.7\%$ ), indicating high sensitivity to  $N_2O$ . Energetic results reveal that  $N_2O$  is physically adsorbed on pristine  $B_{12}N_{12}$  ( $E_{ads} = -0.16$  eV), whereas it interacts moderately with the  $Y@b_{66}$  nanocage ( $E_{ads} = -1.07$  eV), showing an appropriate recovery time ( $\tau = 120.54$  s). In addition, the  $Y@b_{66}$  system demonstrated good selectivity toward  $N_2O$  in the presence of interfering gases ( $H_2$ ,  $CH_4$ , and  $CO$ ). These findings indicate that the  $Y@b_{66}$  nanocage is a promising material for application as a selective  $N_2O$  gas sensor.

**Keywords:**  $B_{12}N_{12}$  nanocage, adsorption,  $N_2O$ , sensor.

## Resumo

A emissão de óxido nitroso ( $N_2O$ ) representa um sério desafio ambiental devido à sua contribuição para a destruição da camada de ozônio. Neste trabalho, cálculos baseados na Teoria do Funcional da Densidade com correção de dispersão (DFT-D3), utilizando o funcional B3LYP e o conjunto de base LanL2DZ, foram realizados para investigar a adsorção de  $N_2O$  em nanogaiolas de  $B_{12}N_{12}$  puras e modificadas com ítrio (Y). Foram analisados os parâmetros geométricos, eletrônicos e energéticos, bem como a sensibilidade eletrônica dos sistemas à adsorção do gás. A nanogaiola  $Y@b_{66}$  apresentou a maior variação do gap de energia ( $\Delta E_{gap} = 38,7\%$ ), indicando elevada sensibilidade ao  $N_2O$ . Os resultados energéticos revelam que o  $N_2O$  se adsorve fisicamente na  $B_{12}N_{12}$  pura ( $E_{ads} = -0,16$  eV), enquanto interage de forma moderada com a nanogaiola  $Y@b_{66}$  ( $E_{ads} = -1,07$  eV), exibindo um tempo de recuperação adequado ( $\tau = 120,54$  s). Além disso, o sistema  $Y@b_{66}$  demonstrou boa seletividade em relação a gases interferentes ( $H_2$ ,  $CH_4$  e  $CO$ ). Esses resultados indicam que a nanogaiola  $Y@b_{66}$  é um material promissor para aplicação como sensor seletivo de  $N_2O$ .

**Palavras-chave:** Nanogaiola  $B_{12}N_{12}$ , adsorção,  $N_2O$ , sensor.

## 1. Introduction

The mission of scientists to find materials capable of detecting or eliminating harmful gases present in the atmosphere has not been an easy task. In recent decades, studies have intensified for the development of chemical sensors capable of rapid and efficient detection of these gases [1,2]. Nanometric materials have been investigated as an alternative for application as sensors, due to their small size, good precision and excellent reactivity properties. Among these materials, we have boron nitride  $(BN)_n$  nanocages, which have gained prominence

due to their excellent properties, such as oxidation resistance, high sensitivity and low recovery time [3].

Even with their excellent properties, some gases, such as  $\text{COCl}_2$ ,  $\text{H}_2\text{S}$ ,  $\text{NO}$  tend not to be spontaneously adsorbed on the surface of the  $\text{B}_{12}\text{N}_{12}$  nanocage [4]. In this context, recent studies have investigated the structural modification of this nanomaterial using transition metals; in order to overcome this limitation, as well as improve their adsorption properties [5, 6]. Among the second-row transition metals, yttrium (Y) has gained prominence in studies as a modifier of nanomaterials for application as a sensor of atmospheric gases [7, 8]. Agwamba et al. [9] investigated the adsorption of metal-doped silicon nanocages ( $\text{Si}_{59}\text{X}$ ;  $\text{X} = \text{Nb}, \text{Mo}, \text{Y}, \text{Zr}$ ) as N-Nitrosodimethylamine (NDMA) gas nanosensors using correlation-exchange functional (PBE) and Lanl2DZ basis set. The results reported that doping with transition metals (Nb, Mo, Y, Zr) in the  $\text{Si}_{60}$  fullerene nanostructure significantly improved the interaction with NDMA. Other molecular descriptors also indicated positive results, confirming the suitability of the surfaces for NDMA detection.

The objective of this study was to explore, using DFT calculations, the adsorption behavior of  $\text{N}_2\text{O}$  gas on Y-modified  $\text{B}_{12}\text{N}_{12}$  nanocages, along with the interfering gases  $\text{H}_2$ ,  $\text{CH}_4$ , and  $\text{CO}$ , to assess the potential of this material as an environmental sensor for toxic gases.

## 2. Computational Methodology

DFT calculations were performed using the ORCA 5.0 program [10]. The pure and Y-modified  $\text{B}_{12}\text{N}_{12}$  nanocages were optimized using the B3LYP-D3 [11] functional and the Lanl2DZ basis set. The B3LYP functional-Grimme D3 dispersion correction/LANL2DZ basis set level of theory was adopted in this study due to its suitable balance between computational cost and reliability for investigating geometric parameters, adsorption energies, and electronic properties of B–N-based nanocage systems. The B3LYP functional has been widely applied in similar adsorption studies, while the D3 dispersion correction improves the description of long-range van der Waals interactions that are relevant in adsorption processes. For the yttrium atom, the LANL2DZ basis set was selected because it incorporates

effective core potentials (ECPs), enabling an efficient treatment of heavier atoms while maintaining methodological consistency across all investigated systems. This computational approach has also been frequently reported in previous studies involving transition-metal-modified nanomaterials. Frequency analysis was performed to confirm the global minima of the optimized structures. The modification of  $B_{12}N_{12}$  with Y resulted in five optimized structures [12]: doped ( $YB_{11}N_{12}$  and  $B_{12}N_{11}Y$ , with substitution of a boron atom and a nitrogen atom for a Y atom in the nanocage, respectively); decorated ( $Y@b_{64}$  and  $Y@b_{66}$ , with a Y atom positioned above the atomic bond between the tetragonal and hexagonal rings and above the atomic bond between two hexagonal rings, respectively) and the encapsulated structure ( $Y@B_{12}N_{12}$ , in which a Y atom is positioned inside the  $B_{12}N_{12}$  nanocage). In the present work, the isolated nanocages (pristine and Y-modified) and the closed-shell gas molecules ( $N_2O$ ,  $H_2$ ,  $CH_4$ , and  $CO$ ) were treated in their singlet ground states, which is the expected configuration for these species. For the adsorbed systems, the calculations were also predominantly performed assuming a singlet state. Additionally, spin-polarized calculations were considered for the  $Y@b_{66}$  system, as indicated by the reference to the  $\alpha$ -spin state in the manuscript, using an unrestricted formalism to allow for possible spin-density redistributions induced by adsorption. The obtained results did not reveal significant electronic changes that would justify the need for a systematic exploration of other spin multiplicities. Therefore, the adopted methodological strategy represents an appropriate balance between theoretical rigor and computational feasibility and is sufficient to consistently describe the adsorption phenomena discussed in this study.

The structures were calculated as neutral, and their stability was investigated through the cohesive energy ( $E_{coh}$ ), which was calculated according to the following equation [13]:

$$E_{coh} = \frac{1}{N} (E_{nanocage} - xE_B - yE_N - zE_{TM}), \quad (1)$$

where  $E_{nanocage}$  is the total energy of the nanocage (either pure or yttrium-modified);  $E_B$ ,  $E_N$  and  $E_Y$  are the energies of the B, N, and Y atoms, respectively; x,

y, and z represent the quantities of each atom (B, N, and Y, respectively) in the structure; and N is the total number of atoms in the nanocage.

Given the energy gap ( $E_{gap}$ ), defined as the difference between the LUMO ( $E_{LUMO}$ ) and HOMO ( $E_{HOMO}$ ) energies, we determine the value of electronic sensitivity ( $\Delta E_{gap}$ ) for the interaction between the  $N_2O$  molecule and the pure or Y-modified  $B_{12}N_{12}$  nanocages according to equation 2, below:

$$\Delta E_{gap} = \left[ \frac{(E_{gap(nanocage-N_2O)} - E_{gap(nanocage)})}{E_{gap(nanocage)}} \right] \times 100\%, \quad (2)$$

where  $E_{gap(nanocage-N_2O)}$  is the energy gap for the interaction of  $N_2O$  with pure and modified  $B_{12}N_{12}$  nanocages, and  $E_{gap(nanocage)}$  is the energy gap for pure or Y-modified  $B_{12}N_{12}$ .

The  $E_{ads}$  value for the interaction between  $N_2O$  and  $B_{12}N_{12}$  or Y- $B_{12}N_{12}$  was calculated according to equation 3:

$$E_{ads} = E_{(nanocage-N_2O)} - (E_{(nanocage)} + E_{(N_2O)}) + E_{BSSE} \quad (3)$$

where  $E_{(nanocage-N_2O)}$  is the energy of the  $B_{12}N_{12}$  or Y- $B_{12}N_{12}$  nanocage bound to  $N_2O$ ,  $E_{(nanocage)}$  is the energy of the pure  $B_{12}N_{12}$  or Y-modified  $B_{12}N_{12}$  nanocages,  $E_{(N_2O)}$  is the energy of the  $N_2O$  molecule, and  $E_{BSSE}$  is the basis set superposition error (BSSE) [13].

The recovery time ( $\tau$ ), which is exponentially related to the system  $E_{ads}$ , can be calculated by equation 4 [14]:

$$\tau = v_0^{-1} e^{-E_{ads}/k_B T} \quad (4)$$

where  $v_0$  is the attempt frequency ( $10^{12} v_0 s^{-1}$ ),  $k_B$  is the Boltzmann constant ( $8.62 \times 10^{-5} eV K^{-1}$ ), and  $T$  is the thermodynamic temperature (K).

The yttrium-modified nanocage that showed the best result for  $N_2O$  detection was subjected to interaction with other gases considered interferents ( $H_2$ ,  $CH_4$  and  $CO$ ) to investigate its selectivity for  $N_2O$  adsorption in comparison with these gases. The selectivity was evaluated by calculating the sensor response (S) and the selectivity coefficient ( $\kappa$ ) using the following equations 5 and 6 [15]:

$$S = \frac{|R_{\text{gas}} - R_{\text{pure}}|}{R_{\text{pure}}} = \frac{\left| \frac{1}{\sigma_{\text{gas}}} - \frac{1}{\sigma_{\text{pure}}} \right|}{\frac{1}{\sigma_{\text{pure}}}} = \frac{|\sigma_{\text{pure}} - \sigma_{\text{gas}}|}{\sigma_{\text{gas}}}, \quad (5)$$

$$\kappa_{N_2O-int} = \frac{S_{N_2O}}{S_{int}}, \quad (6)$$

where  $\sigma_{\text{gas}}$  represents the conductivity of the gas adsorbed on the surface of the nanocage,  $\sigma_{\text{pure}}$  is the conductance of the isolated nanocage (equation 5). In equation 6,  $S_{N_2O}$  and  $S_{int}$  indicate sensitivity to  $N_2O$  gas and to interferents gases, respectively, and  $\kappa_{N_2O-int}$  represents the sensitivity ratio to  $N_2O$  against an interfering gas.

### 3. Results and Discussion

The optimized structures of  $B_{12}N_{12}$  and Y-modified nanocages are shown in Fig. 1 a), and their electronic properties are presented in Table 1. The interaction of  $N_2O$  gas is presented in Fig. 1 b). The results show that for  $B_{12}N_{12}$  nanocages, the B-N bond lengths of 1.485 and 1.437 Å are in agreement with previous studies [16, 17].

As seen in Fig. 1 a), the modification with Y atom causes a local deformation in the nanocages and this may be due to their large atomic radius. After the optimization of the geometry of the modified cages, it is observed that there was an increase in the bond length; in the case of the encapsulated structure, the metal projected to the center of the nanocage. Fig. 1 b) shows that  $N_2O$  presents a nonlinear geometry when interacting with Y in the decorated nanocages, binding through the N atom and not through O as occurs in other analyzed systems.

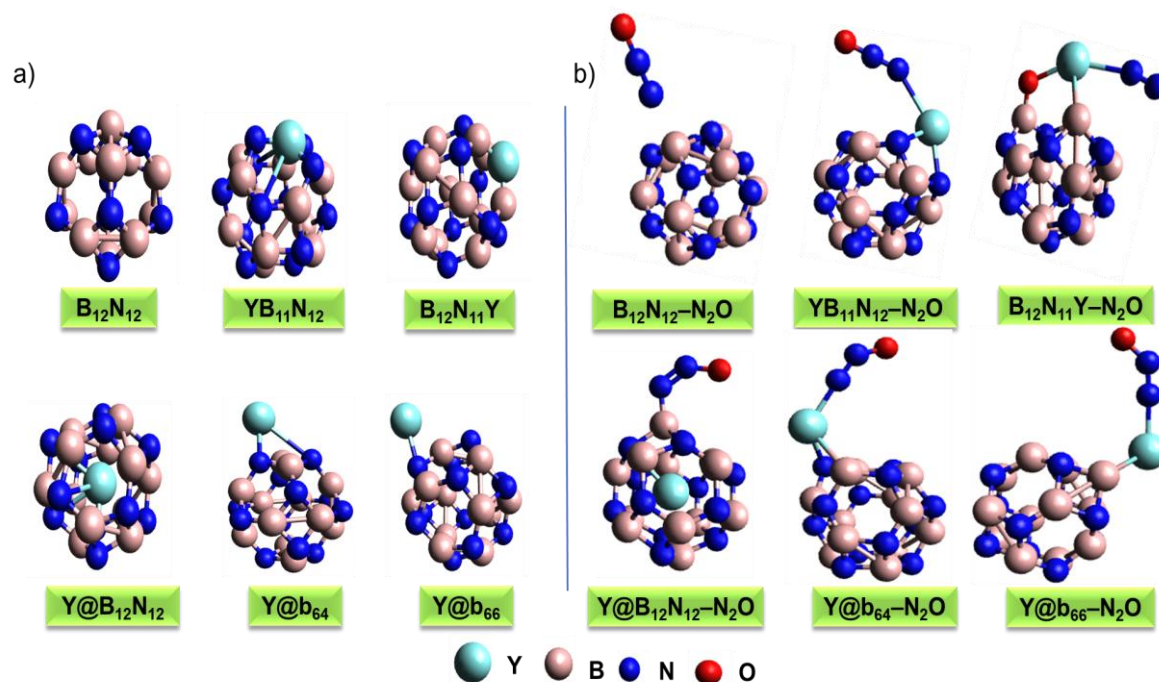


Figure 1. Optimized structures of pristine and Y-modified B<sub>12</sub>N<sub>12</sub> nanocages (a), and adsorption configurations of the N<sub>2</sub>O molecule on isolated and Y-modified B<sub>12</sub>N<sub>12</sub> nanocages (b).

Table 1 shows the cohesion energy ( $E_{\text{coh}}$ ), dipole moment (DM) and charge transfer (Q) for the pure and Y-modified B<sub>12</sub>N<sub>12</sub> structures. The B<sub>12</sub>N<sub>12</sub> nanocage showed a dipole moment equal to zero [18]. The highest dipole moment value was for B<sub>11</sub>N<sub>12</sub>Y DM = 10.18 Debye, while the lowest was for Y@B<sub>12</sub>N<sub>12</sub> DM = 1.63 Debye, indicating a lower charge partition in the encapsulated cage (-0.37 |e|). The largest charge shift from Y to the cage is seen in the Y@b<sub>64</sub> system (+0.45 |e|), where the metal replaces a B atom in B<sub>12</sub>N<sub>12</sub>. The  $E_{\text{coh}}$  analysis provides information about the affinity of the nanocage with the metal, exploring in detail the stability of the cage/metal systems. The results show that the lower  $E_{\text{coh}}$  values (less negative) for the modified nanocages prove that all structures are less stable than pure B<sub>12</sub>N<sub>12</sub> [12]. In addition, YB<sub>11</sub>N<sub>12</sub> stands out as the most unstable among the studied nanocages, with  $E_{\text{coh}} = -6.81$  eV.

The parameters of the isolated and modified systems for N<sub>2</sub>O gas adsorption: HOMO energy ( $E_{\text{H}}$  / eV), LUMO energy ( $E_{\text{L}}$  / eV), HOMO-LUMO gap ( $E_{\text{gap}}$  / eV), sensitivity ( $\Delta E_{\text{gap}}$  / %) are shown in Table 2. It is noted that the energies

of the HOMO and LUMO orbitals of  $B_{12}N_{12}$  underwent changes after the interaction with  $N_2O$ , this change directly reflected in the variation of  $E_{gap}$ .

Table 1 - Calculated cohesive energy ( $E_{coh}$ ), dipole moment (DM), and yttrium atomic charges (Q) for the isolated systems.

System	$E_{coh}$ / eV	DM / Debye	Q /  e
$B_{12}N_{12}$	- 6.82	0.00	-
$YB_{11}N_{12}$	- 6.81	10.18	+0.63
$B_{12}N_{11}Y$	- 6.49	9.71	+0.05
$Y@b_{64}$	- 6.64	6.93	+0.45
$Y@b_{66}$	- 6.63	7.21	+0.33
$Y@B_{12}N_{12}$	- 6.27	1.63	-0.37

The bandgap of  $B_{12}N_{12}$  decreased from 5.93 eV to 5.18 eV after adsorption, indicating weak interaction with  $N_2O$  gas. The sensitivity of a system is determined by the change in the bandgap before and after gas adsorption (see Equation 2) [19, 20]. In this context, modifying the nanocage with yttrium increases its sensitivity to the gas [21]. For the pure  $B_{12}N_{12}$  system, the sensitivity to  $N_2O$  adsorption was ( $\Delta E_{gap} = 12.54\%$ ). These data are confirmed by the low adsorption energy obtained for the system ( $E_{ads} = -0.16$  eV), characterizing a physisorption ( $E_{ads} > -0.3$  eV) [22] with Van der Waals-type interaction. Among the metal-modified cages,  $B_{12}N_{11}Y$  showed the lowest sensitivity ( $\Delta E_{gap} = 7.42\%$ ) with adsorption energy ( $E_{ads} = -0.55$  eV). In the case of the  $Y@b_{66}$  ( $\alpha$  - spin up) system, the energy was ( $E_{ads} = -1.07$  eV), a value considered moderate for a chemisorption process.

Table 2 – Calculated parameters for the isolated nanocages and their interaction with N<sub>2</sub>O, including HOMO energy (E<sub>H</sub>), LUMO energy (E<sub>L</sub>), energy gap (E<sub>gap</sub>), electronic sensitivity ( $\Delta E_{\text{gap}}$ ), and adsorption energy (E<sub>ads</sub>).

System	S	Isolated			With N <sub>2</sub> O adsorbed				
		E <sub>H</sub> (eV)	E <sub>L</sub> (eV)	E <sub>gap</sub> (eV)	E <sub>H</sub> (eV)	E <sub>L</sub> (eV)	E <sub>gap</sub> (eV)	$\Delta E_{\text{gap}}$ (%)	E <sub>ads</sub> (eV)
B <sub>12</sub> N <sub>12</sub>	S	-7.77	-1.84	5.93	-7.61	-2.43	5.18	12.54	-0.16
YB <sub>11</sub> N <sub>12</sub>	$\alpha$	-6.71	-2.78	3.93	-6.60	-3.33	3.27	16.87	-0.46
B <sub>12</sub> N <sub>11</sub> Y	$\alpha$	-5.48	-2.79	2.69	-5.65	-3.16	2.49	7.42	-0.55
Y@b <sub>64</sub>	$\alpha$	-4.53	-2.19	2.34	-5.99	-2.91	3.08	31.44	-0.63
	$\beta$	-5.70	-2.63	3.07	-5.99	-3.35	2.64	14.12	
Y@b <sub>66</sub>	$\alpha$	-4.57	-2.20	2.37	-6.16	-2.87	3.29	38.70	-1.07
	$\beta$	-5.33	-2.72	2.61	-6.47	-3.32	3.15	20.53	
Y@B <sub>12</sub> N <sub>12</sub>	$\alpha$	-4.88	-2.89	1.99	-4.87	-3.33	1.54	22.21	-0.49
	$\beta$	-5.00	-2.85	2.15	-5.19	-3.34	1.85	14.19	

$\alpha$  – spin up – (alpha);  $\beta$  – spin down – (beta)

Furthermore, it showed good sensitivity ( $\Delta E_{\text{gap}} = 38.70\%$ ) with satisfactory recovery time at a temperature of 298 K ( $\tau = 120.54$  s), making it suitable as a material for application as a sensor. To assess the selectivity of the Y@b<sub>66</sub> nanocage for N<sub>2</sub>O gas detection, the adsorption of other gases, including H<sub>2</sub>, CH<sub>4</sub>, and CO, was examined using the same calculation methods. The optimized structures are presented in Fig. 2.

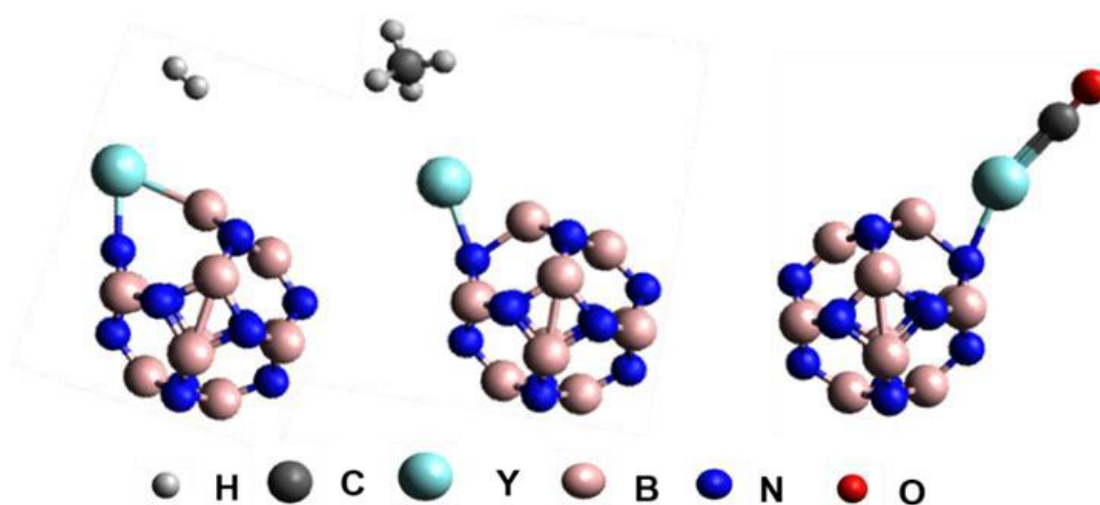


Figure 2. Optimized adsorption configurations of interfering gases ( $H_2$ ,  $CH_4$ , and  $CO$ ) on the  $Y@b_{66}$  nanocage.

Table 3 presents the results for HOMO-LUMO ( $E_{gap}$ ), distance ( $d$ ), adsorption energy ( $E_{ads}$ ) and sensitivity ( $\Delta E_{gap}$ ) for the adsorption of  $H_2$ ,  $CH_4$  and  $CO$  gases (considered interfering gases) on the surface of the  $Y@b_{66}$  nanocage. The selection of interfering gases ( $H_2$ ,  $CH_4$ , and  $CO$ ) was based on their practical relevance and frequent presence in environments where  $N_2O$  detection may occur. These gases commonly coexist with  $N_2O$  in industrial, environmental, and atmospheric contexts and may interfere with its detection. Additionally, their distinct physicochemical properties, such as polarity, molecular size, and reactivity, allow for a broader evaluation of the sensor's selectivity under realistic conditions.

The FMO data show that the nanocage is more sensitive to nitrous oxide compared to the other gases studied ( $\Delta E_{gap} = 38.70\%$ ), indicating that  $N_2O$  is preferentially detected by the  $Y@b_{66}$  system. Regarding the adsorption distances of the interfering gases on the nanocage, it is noted that  $CH_4$  has the largest interaction distance ( $d = 3.44 \text{ \AA}$ ), while the smallest was observed for  $N_2O$  gas ( $d = 2.16 \text{ \AA}$ ). The adsorption energies indicate that  $H_2$ ,  $CH_4$  and  $CO$  gases undergo physical adsorption on the surface of the  $Y@b_{66}$  cage [23]. For nitrous oxide gas adsorption, the resulting adsorption energy ( $E_{ads} = -1.07 \text{ eV}$ ) characterizes a chemisorption process. Regarding the recovery time of the interfering gases, the values obtained were high, making them unfavorable for adsorption on the  $Y@b_{66}$  surface. In contrast, the recovery time for the interaction between the nanocage and  $N_2O$  gas ( $\tau = 120.54 \text{ s}$ ) is considered satisfactory at room temperature (however, this result should be considered only as a preliminary theoretical estimate, and experimental validation is required to confirm the practical recovery performance of the proposed material). The preference of the  $Y@b_{66}$  nanocage for  $N_2O$  results from a combination of electronic and structural factors. The yttrium atom creates a highly polarized electrophilic site, favoring interaction with  $N_2O$ , which exhibits an asymmetric electronic distribution. Adsorption occurs mainly through  $\sigma$ -donation from  $N_2O$  to the metal center, with possible  $\pi$ -back-donation, enhancing charge transfer and characterizing a moderate chemisorption process.

To analyze the interaction of Y@b<sub>66</sub> with N<sub>2</sub>O and interfering gases, the sensitivity (S) and selectivity ( $\kappa$ ) were calculated using the same methodology as in previous studies.

Table 3 – Values of gap HOMO-LUMO ( $E_{\text{gap}}$ ), cage/gas distance (d), adsorption energy ( $E_{\text{ads}}$ ), electronic sensitivity ( $\Delta E_{\text{gap}}$ ), recovery time ( $\tau$ ), and also the sensitivity (S) and selectivity coefficient ( $\kappa$ ) calculated for the interaction of H<sub>2</sub>, CH<sub>4</sub> and CO gases with the Y@b<sub>66</sub> cage.

System	$E_{\text{gap}}$ (eV)	d (Å)	$E_{\text{ads}}$ (eV)	$\Delta E_{\text{gap}}$ (%)	$\tau$	S	$\kappa$
Y@b <sub>66</sub> – N <sub>2</sub> O	3.29	2.16	-1.07	38.70	120.54 s	$5.93 \times 10^7$	—
Y@b <sub>66</sub> – H <sub>2</sub>	2.30	3.01	-0.19	3.04	$1.13 \times 10^{12}$ s	2.90	$2.05 \times 10^7$
Y@b <sub>66</sub> – CH <sub>4</sub>	2.38	3.44	-0.04	0.34	$1.24 \times 10^{19}$ s	0.22	$2.69 \times 10^8$
Y@b <sub>66</sub> – CO	1.79	2.09	-0.60	24.54	$5.15 \times 10^5$ s	$7.95 \times 10^4$	$7.46 \times 10^2$

These parameters assess the system's effectiveness in gas detection and its ability to distinguish a specific gas in the atmosphere. Overall, the results indicate that the Y@b<sub>66</sub> nanocage exhibits higher sensitivity to N<sub>2</sub>O compared to other gases and can effectively differentiate it from interfering gases, showing the highest selectivity coefficient for the N<sub>2</sub>O/CH<sub>4</sub> pair. These findings suggest that the Y@b<sub>66</sub> nanocage holds potential as a sensor with strong sensitivity and selectivity for N<sub>2</sub>O detection.

Table 4 presents the performance of different materials for N<sub>2</sub>O gas adsorption, based on previously reported studies in the literature [24–27], along with the results obtained for the Y@b<sub>66</sub> nanocage. It is observed that Y@b<sub>66</sub> exhibits higher sensitivity toward N<sub>2</sub>O ( $\Delta E_{\text{gap}} = 38.70\%$ ) compared to the other analyzed systems.

The results obtained for the B<sub>12</sub>N<sub>12</sub> nanocage indicate an adsorption energy typical of a physisorption process ( $E_{\text{ads}} = -0.22$  eV), evidencing a weak interaction between the cage surface and the N<sub>2</sub>O molecule, which suggests limited efficiency for sensing applications. In contrast, structural modification with the yttrium metal promotes significant changes in the electronic and reactive properties of the system, favoring a stronger interaction with the gas.

In fact, the Y@b<sub>66</sub> nanocage exhibits a pronounced sensitivity ( $\Delta E_{\text{gap}} = 38.70\%$ ), along with a more negative adsorption energy ( $E_{\text{ads}} = -1.07$  eV), characteristic of a chemisorption process. This behavior indicates the formation of stronger chemical interactions, resulting in greater charge transfer and, consequently, a more significant electronic response of the material.

Table 4 - Comparison of the detection performance between Y@b<sub>66</sub> and previously reported materials in the literature.

Sensor	Functional	$E_{\text{ads}} / \text{eV}$	$\Delta E_{\text{gap}} / (\%)$	References
B <sub>12</sub> N <sub>12</sub>	B3LYP	-0.22	34.95	[24]
B <sub>35</sub>	B3LYP	-0.13	0.20	[25]
Be <sub>12</sub> O <sub>12</sub>	B3LYP-D3	-0.42	20.99	[26]
Mg <sub>12</sub> O <sub>12</sub>	B3LYP-D3	-0.53	1.44	[26]
Al-doped graphene	B3LYP	-0.23	15.91	[27]
Zn <sub>12</sub> O <sub>12</sub>	B3LYP	-0.70	19.80	[28]
B-SnS <sub>2</sub>	PBE	-2.20	26.32	[29]
Mo-WSe <sub>2</sub>	PBE	-2.85	16.37	[30]
Y@b <sub>66</sub>	B3LYP-D3	-1.07	38.70	This work

Furthermore, the larger variation in the energy gap suggests superior performance in sensing applications, since small structural changes induced by gas adsorption generate detectable responses. Therefore, it can be concluded that the Y@b<sub>66</sub> nanocage stands out as a promising material for the development of highly sensitive and selective sensors, with strong potential for the rapid and efficient detection of N<sub>2</sub>O gas.

#### 4. Conclusions

In summary, Y-modified nanocages exhibited improved theoretical performance compared to pristine B<sub>12</sub>N<sub>12</sub> for N<sub>2</sub>O adsorption. Among the investigated systems, the Y@b<sub>66</sub> nanocage presented the most favorable adsorption energy, electronic sensitivity, and selectivity toward N<sub>2</sub>O molecules among the analyzed structures. These computational findings suggest that Y@b<sub>66</sub> may represent a promising theoretical candidate for future studies involving selective N<sub>2</sub>O sensing applications. Nevertheless, the present results are based exclusively on theoretical calculations, and further experimental investigations are still required to evaluate synthesis feasibility, long-term stability, environmental effects, and practical sensor performance under real operating conditions before any definitive technological application can be established.

### Data Availability Statement

The data that support the findings of this study are available from the corresponding author upon reasonable request.

### Conflicts of Interest

The authors declare no conflicts of interest.

### Funding

This study was supported by FAPEMA - Foundation for Research and Scientific and Technological Development of Maranhão, project number BD-05177/23.

### Acknowledgments

This work has been supported by the following Brazilian research agencies: National Council for Scientific and Technological Development (CNPq), 304205/2018-4, National Council for the Improvement of Higher Education (CAPES), Finance Code 001, Maranhão Research and Scientific and Technological

Development Support Foundation (FAPEMA). The first author received fellowships from FAPEMA BD-05177/23.

## References

- [1] Yoosefian M (2017) Powerful greenhouse gas nitrous oxide adsorption onto intrinsic and Pd doped Single walled carbon nanotube, *Appl. Surf. Sci.* 392:225–230.
- [2] Rad AS (2015) First principles study of Al-doped graphene as nanostructure adsorbent for NO<sub>2</sub> and N<sub>2</sub>O: DFT calculations, *Appl. Surf. Sci.* 357:1217–1224.
- [3] Ding S, Gu W (2022) Evaluate the potential utilization of B<sub>24</sub>N<sub>24</sub> fullerene in the recognition of COS, H<sub>2</sub>S, SO<sub>2</sub>, and CS<sub>2</sub> gases (environmental pollution), *J. Mol. Liq.* 345:117041.
- [4] Silva ALP, Sousa NS, Varela JJG (2023) Theoretical studies with B<sub>12</sub>N<sub>12</sub> as a toxic gas sensor: a review, *J. Nanopart. Research* 25:22.
- [5] Qadir KW, Mohammadi MD, Ridha NJ, Abdullah HY (2024) Determining the binding mechanism of B<sub>12</sub>N<sub>12</sub>(Zn) with CH<sub>4</sub>, CO, CO<sub>2</sub>, H<sub>2</sub>O, N<sub>2</sub>, NH<sub>3</sub>, NO, NO<sub>2</sub>, O<sub>2</sub>, and SO<sub>2</sub> gases, *Microp. Mesop. Mater.* 379:113289.
- [6] Sousa NS, Nascimento WCL, Silva ALP, Varela JJG (2024) DFT study of TM (Sc-Zn) modified B<sub>12</sub>N<sub>12</sub> nanocage as sensor for N<sub>2</sub>O gas selective detection. *Sens Actuat A* 378:115841.
- [7] Nascimento WCL, Sousa NS, Silva ALP, Maciel AP (2026) Yttrium-Modified B<sub>12</sub>N<sub>12</sub> Nanocages for High-Performance H<sub>2</sub> Sensing: Insights from DFT Calculations on Sensitivity, Selectivity, and Recovery, *ACS Omega* 11:6421-6433.

- [8] Esrafil MD, Sadeghi SY (2022) decorated all-boron B<sub>38</sub> nanocluster for reversible molecular hydrogen storage: A first-principles investigation, *Int. J. Hydrog. Energy* 47:11611–11621.
- [9] Agwamba EC, Mathias GE, Louis H, Ikenyirimba O, Unimuke TO, Ahuekwe et al. Single (2023) metal-doped silicon (Si<sub>59</sub>X; X = Nb, Mo, Y, Zr) nanostructured as nanosensors for N-Nitrosodimethylamine (NDMA) pollutant: Intuition from computational study, *Mater. Today Commun.* 35:106173.
- [10] Neese F (2022) Software update: The ORCA program system–Version 5.0. *WIREs, Comput. Mol. Sci.* 12:e1606.
- [11] Grimme S (2011) Density functional theory with London dispersion corrections. *WIREs, Comput. Mol. Sci.* 1:211–228.
- [12] Silva ALP, Varela JJG (2023) Density Functional Theory Study of Cu-Modified B<sub>12</sub>N<sub>12</sub> Nanocage as a Chemical Sensor for Carbon Monoxide Gas, *Inorg Chem.* 62:1926–1934.
- [13] Silva ALP, Varela JJG (2024) MB<sub>11</sub>N<sub>12</sub> (M = Fe–Zn) Nanocages for Cyanogen Chloride Detection: A DFT Study. *J. Inorg. Organom. Polym. Mat.* 34:302–312.
- [14] Koettgen J, Zacherle T, Grieshammer S, Martin M (2017) Ab initio calculation of the attempt frequency of oxygen diffusion in pure and samarium doped ceria. *Phys. Chem. Chem. Phys.* 19:9957-9973.
- [15] Cui H, Jia P, Peng X, Li P (2020) Adsorption and sensing of CO and C<sub>2</sub>H<sub>2</sub> by S-defected SnS<sub>2</sub> monolayer for DGA in transformer oil: A DFT study. *Mater. Chem. Phys.* 249:123006.
- [16] Rad AS, and Ayub K (2017) O<sub>3</sub> and SO<sub>2</sub> sensing concept on extended surface of B<sub>12</sub>N<sub>12</sub> nanocages modified by Nickel decoration: A comprehensive DFT study *Solid State Sci.* 69:22–30.
- [17] Ma S, Li D, Rao X, Xia X, Su Y, Lu Y (2020) Pd-doped h-BN monolayer: a promising gas scavenger for SF<sub>6</sub> insulation devices. *Adsorption* 26:619-626.

- [18] Escobedo-Morales A, Tepech-Carrillo L, Bautista-Hernández A, Camacho-García JH, Cortes-Arriagada D, Chigo-Anota, E. (2019) Effect of Chemical Order in the Structural Stability and Physicochemical Properties of B<sub>12</sub>N<sub>12</sub> Fullerenes. *Sci. Rep.* 9:16521.
- [19] Baei MT (2013) Si-Doped B<sub>12</sub>N<sub>12</sub> Nanocage as an Adsorbent for Dissociation of N<sub>2</sub>O to N<sub>2</sub> Molecule. *Heteroatom Chem.* 24:476-481.
- [20] Sousa NS, Silva ALP, Nascimento WCL, Martins J dos Santos, Bezerra CWB (2025). Theoretical Study of Ni-Modified B<sub>12</sub>N<sub>12</sub> Nanocages: Insights into CO Capture Potential. *Microporous and Mesoporous Materials*, 113823.
- [21] Nascimento WCL, Sousa NS, Martins J dos S, Maciel AP (2024) Estudo a Nível DFT do B<sub>12</sub>N<sub>12</sub> Puro e Modificado com Y para Adsorção do Gás Hidrogênio. *Anais do Congresso Brasileiro de Química - CBQ 63º edição.*
- [22] Hadipour NL, Peyghan AA, Soleymanabadi H (2015) Theoretical Study on the Al-Doped ZnO Nanoclusters for CO Chemical Sensors. *J. Phys. Chem. C* 119:6398–6404.
- [23] Choir AA, Amelia SR, Martoprawiro MA, Kusumawati Y, Ivansyah AL (2024) Insight into the adsorption properties of CO<sub>2</sub> and H<sub>2</sub> gas on the B<sub>12</sub>Y<sub>12</sub> (Y - N, P, As, Sb) nanocages from host-guest interaction perspective. *Int. J. Hydrog. Energy* 53:780–791.
- [24] Baei MT, Ghasemi AS, Lemeski ET, Soltani A, Gholami N (2016) BN Nanotube Serving as a Gas Chemical Sensor for N<sub>2</sub>O by Parallel Electric Field. *J. Clust. Sci.* 27:1081–1096.
- [25] Hossain MdA, Hossain MdR, Hossain MdK, Khandaker JI, Ahmed F, Ferdous T, Hossain Md A (2020) An ab initio study of the boron nanocluster for application as atmospheric gas (NO, NO<sub>2</sub>, N<sub>2</sub>O, NH<sub>3</sub>) sensor. *Chem. Phys. Lett.* 754:137701.
- [26] Sajid H, Siddique SA, Ahmed E, Arshad M, Gilani MA, Rauf A, Imran M, Mahmood T (2022) DFT outcome for comparative analysis of Be<sub>12</sub>O<sub>12</sub>, Mg<sub>12</sub>O<sub>12</sub> and

Ca<sub>12</sub>O<sub>12</sub> nanocages toward sensing of N<sub>2</sub>O, NO<sub>2</sub>, NO, H<sub>2</sub>S, HCN and SO<sub>3</sub> gases, Comput. Theor. Chem. 1211:113694.

[27] Rad AS (2015) First principles study of Al-doped graphene as nanostructure adsorbent for NO<sub>2</sub> and N<sub>2</sub>O: DFT calculations, Appl. Surf. Sci. 357:1217–1224.

[28] Beheshtian J, Peyghan AA, Bagheri Z (2012) Adsorption and dissociation of Cl<sub>2</sub> molecule on ZnO nanocluster. Appl. Surf. Sci. 258:8171–8176.

[29] Hang A, Dong A, Gui Y (2022) Gas-sensing properties of B/N-modified SnS<sub>2</sub> monolayer to greenhouse gases (NH<sub>3</sub>, Cl<sub>2</sub>, and C<sub>2</sub>H<sub>2</sub>). Mat. 15(15):5152–5152.

[30] Cheng S, Chen J, Zeng W, Zhou Q (2023) The adsorption and sensing mechanism of toxic gases HCN, NO<sub>2</sub>, NH<sub>3</sub> and Cl<sub>2</sub> on Mo, Ag-modified WSe<sub>2</sub> monolayer: insights from the first-principles computations. Mater. Today Commun. 35:105906.